Robotica: (2021) volume 39, pp. 1181–1201. © The Author(s), 2020. Published by Cambridge University Press.
doi:10.1017/S0263574720001009

Polynomial-Based Robust Adaptive Impedance Control of Electrically Driven Robots

Alireza Izadbakhsh†* and Saeed Khorashadizadeh‡

†*Department of Electrical Engineering, Garmsar branch, Islamic Azad University, Garmsar, Iran*
‡*Faculty of Electrical and Computer Engineering, University of Birjand, Birjand, Iran*

(Accepted September 29, 2020. First published online: November 4, 2020)

SUMMARY
This paper presents a robust adaptive impedance controller for electrically driven robots using polynomials of degree N as a universal approximator. According to the universal approximation theorem, polynomials of degree N can approximate uncertainties including un-modeled dynamics and external disturbances. This fact is completely discussed and proved in this paper. The polynomial coefficients are estimated based on the adaptive law calculated in the stability analysis. A performance evaluation has been carried out to verify satisfactory performance of the controller. Simulation results on a two degree of freedom manipulator have been presented to guarantee its successful implementation.

KEYWORDS: Impedance control; Robot manipulator; Function approximation technique; Robust adaptive control; Universal approximation theorem.

1. Introduction

Human's brain as a very advanced and intelligent controller carries out various tasks precisely when it is in contact with environment. Suppose that you want to pick up and move a component. Your brain exactly determines the required force for keeping the component and then tracks a desired trajectory to reach the destination. Furthermore, the brain switches smoothly between position and force control without any problem. This high capability owes to exact recognition of the environment nature by our brain. As a result, there is not considerable uncertainty in the interaction between human and its surrounding environment.

In the last few decades, various interaction control strategies such as hybrid control,[1–3] impedance control[4–6] and hybrid impedance control (HIC)[7,8] for robot manipulators have been proposed based on imitating the human performance. Hybrid position/force control can only control either the position or the force without considering the manipulator impedance.[9] Impedance control is basically a position control scheme in which the manipulator behavior is determined by proper choice of desired impedance parameters. HIC takes the advantages of hybrid position/force control and impedance control to regulate position, force and impedance. However, HIC suffers from switching between controllers. In interaction control problem, manipulator behavior is highly affected by uncertainties in contact with environment. Two aspects of uncertainties include manipulator dynamics and environment properties. Manipulator dynamics is nonlinear, highly coupled and multivariable. In addition, a prefect model is not usually available. Therefore, a nominal model is used for designing control law, while it differs from the actual model. Other face of uncertainty is related to environment, when the environment properties are not available or our information is incomplete. In these situations, regulating impedance parameters is a difficult task. In other words, inaccurate selection of these parameters degrades the controller performance in both transient and steady states.

* Corresponding author. E-mail: izadbakhsh_alireza@hotmail.com

https://doi.org/10.1017/S0263574720001009 Published online by Cambridge University Press

To solve the aforementioned problems, some robust and adaptive approaches based on uncertainty estimation have been proposed. As pointed out in the paper,[10] function approximation methods such as neuro-fuzzy systems,[11–13] Szasz–Mirakyan Operator,[14] differential equations,[15,16] Fourier series expansion and Bernstein polynomials[17–25] have been utilized in robust adaptive control of many nonlinear systems. The Stone–Weierstrass theorem, from the classical real analysis' point of view, can be used to guarantee that these mathematical tools possess the universal approximation property.

In ref. [10], a third-order Taylor series expansion plays the role of uncertainty estimator. The Taylor series coefficients are then tuned based on the adaptation law obtained in the stability analysis. According to ref. [26], such an approximation is not technically correct. The reason is that the second condition of the Stone–Weierstrass theorem is not satisfied for such an approximation. Moreover, the proposed approach in ref. [10] does not give suitable stability analysis for the overall control system. It uses the assumption that the control signal is bounded to prove the stability and boundedness of the closed-loop internal signals. It is worth emphasizing that the controller operation does not influence the plant in the saturated area of the control input, since the actuators are driving the system by their maximum value. In this situation, the tracking error may be unacceptable due to unsatisfactory performance of the controller.[27] Nevertheless, the stability analysis presented in ref. [10] does not address the saturated area properly. Another challenging issue is that in ref. [10], stability is discussed separately in saturated and unsaturated operation areas. However, this stability analysis is not complete and comprehensive, since transitions from saturation area to unsaturated area and vice versa are neglected.

Another considerable point is that Taylor's theorem will only approximate a differentiable function at specific points and can produce a Taylor series that does not converge to the original function. Hence, we need to find a better technique to approximate our nonlinear functions.

This paper presents a robust adaptive impedance controller for electrically driven robots using polynomials of degree N as a universal approximator. In this paper, based on the Stone–Weierstrass theorem, it is proved that these polynomials are universal approximators. The overall closed-loop system is composed of full-actuated robotic manipulator for n degrees of freedom (DOF), and the proposed controller is proved to be uniformly ultimately bounded (UUB) stable. Moreover, a performance evaluation is added to verify satisfactory performance of transient response of the controller.

This paper is organized as follows. Section 2 briefly presents dynamic modeling of the robotic system including the robot manipulator and the permanent magnet DC motors in the task space. In section 3, impedance control is introduced shortly. In section 4, we will see how polynomials can be used to approximate any continuous function with Weierstrass approximation theorem. Section 5 presents the controller design scenario. The stability analysis and performance evaluation are also presented in this section. Simulation results are illustrated in Section 6. Finally, concluding remarks are drawn in section 7. In what follows, we use the notation $\lambda_{\min}(\bullet)$ and $\lambda_{\max}(\bullet)$ to indicate the minimum and maximum eigenvalues, respectively, of a positive definite bounded matrix. The norm of vector $y \in \Re^n$ is defined as $\|y\| = \sqrt{y^T y}$ and that of matrix $\|A(y)\| = \sqrt{\lambda_{\max}(A(y)^T A(y))}$.

2. Dynamic Equation of Electrically Driven Robot

The mathematical dynamics model of a rigid-link electrically driven robot having n-DOF in contact with the environment is described by[28,29]

$$D(q)\ddot{q} + C(q,\dot{q})\dot{q} + g(q) + \tau_d = HI - J^T(q)F_{ext} \tag{1}$$

$$L\dot{I} + RI + K_b\dot{q} = u(t) \tag{2}$$

where q, $\dot{q}$ and $\ddot{q}$ denote the $n \times 1$ vectors of generalized link position, velocity and acceleration, respectively, $D(q) \in \Re^{n\times n}$ is a symmetric positive definite matrix, $C(q,\dot{q})\dot{q} \in \Re^n$ is the vector of Coriolis/centrifugal forces, $g(q) \in \Re^n$ is the vector of gravitational forces, $\tau_d \in \Re^n$ is the vector of external disturbances, $H \in \Re^{n\times n}$ is an invertible constant diagonal matrix characterizing the electro-mechanical conversion between the current vector and the torque vector, $I \in \Re^n$ is the vector of motor armature currents, $J(q) \in \Re^{n\times n}$ is the Jacobian matrix and $F_{ext} \in \Re^n$ is the external force exerted by the robot at the end-effector. The constant positive definite diagonal matrices $L \in \Re^{n\times n}$, $R \in \Re^{n\times n}$ and $K_b \in \Re^{n\times n}$ represent the electrical inductance, the electrical resistance and the back EMF effects,

https://doi.org/10.1017/S0263574720001009 Published online by Cambridge University Press

respectively, of the actuators. Also, $u(t) \in \Re^n$ denotes the control input voltage applied for the joint actuators.

When controlling the dynamic behavior of the end-effector/environment interactions comes to be a main concern, it is often desirable to describe the manipulator dynamics in its operational space. Let $h \in \Re^n$ be a task space vector defined by:[30]

$$h = \phi(q) \tag{3}$$

where $\phi(\bullet) \in \Re^n \rightarrow \Re^n$ is generally a nonlinear transformation describing the relation between the joint space and task space. We can relate the velocities and accelerations in the task space to those in the joint space by the following relations:

$$\dot{h} = J(q)\dot{q} \tag{4}$$

$$\ddot{h} = J(q)\ddot{q} + \dot{J}(q)\dot{q} \tag{5}$$

Now, substituting Eqs. (4) and (5) into Eq. (1), and multiplying both sides by $J(q)^{-T}$ yields

$$M(h)\ddot{h} + C'(h, \dot{h})\dot{h} + G(h) = J(q)^{-T}HI - F_{ext} \tag{6}$$

where

$$M(h) = J(q)^{-T} D(q) J(q)^{-1}$$

$$C'(h, \dot{h}) = J(q)^{-T} \left(C(q, \dot{q}) - D(q)J(q)^{-1}\dot{J}(q)\right) J(q)^{-1}$$

$$G(h) = J(q)^{-T}(g(q) + \tau_d)$$

In these equations, $J(q)^{-T}$ means $(J(q)^T)^{-1}$.

3. Standard Impedance Control

Impedance control utilizes a single control law, which attempts to regulate both position and force by specifying a dynamic relationship between them. This relationship is chosen to be a second-order linear impedance because such systems are well understood and simple to control. A standard impedance control law is shown in Eq. (7), where $M_t \in \Re^{n\times n}$, $B_t \in \Re^{n\times n}$ and $k_t \in \Re^{n\times n}$ are constant positive definite matrices, representing the desired inertia, damping and stiffness matrices in task space. Vectors $h \in \Re^n$ and $h_d \in \Re^n$ represent the actual and the desired end-effector positions, and F_{ext} represents the generalized force the environment exerts upon the end-effector

$$\mathrm{M}_t(\ddot{h} - \ddot{h}_d) + \mathrm{B}_t(\dot{h} - \dot{h}_d) + \mathrm{k}_t(h - h_d) = -F_{ext} \tag{7}$$

The target impedance parameters are specified by the user and have the dimensions of the task space. They cause the manipulator to exhibit the dynamics of a multi-directional mass–spring–damper system. The target impedance matrices are typically chosen to be diagonal, resulting in uncoupled response along each principle direction of h. With this in mind, ref. [31] proposed the standard adaptive impedance controller using function approximation technique (FAT) and introduced the following target impedance

$$\mathrm{M}_t(\ddot{h}_t - \ddot{h}_d) + \mathrm{B}_t(\dot{h}_t - \dot{h}_d) + \mathrm{k}_t(h_t - h_d) = -F_{ext} \tag{8}$$

where $h_t \in \Re^n$ is the state vector of the reference model (8). The FAT-based controller is designed such that h converges to h_t asymptotically, which yields convergence of the new target impedance (8) to (7) as desired. It does not require any knowledge of the system dynamics' parameters, except for the Jacobian matrix and torque constant. However, weighting matrices (Fourier series coefficients) with large dimensions impose a considerable computational load in its real-time implementation. This problem has been improved in ref. [32]. In the next section, we present a simpler FAT-based adaptive impedance controller, for rigid-link electrically driven robot interacting with the environment.

https://doi.org/10.1017/S0263574720001009 Published online by Cambridge University Press

4. Function Approximation Using Polynomials of Degree *N*

Uncertainty estimators are not confined to fuzzy systems and neural networks. Polynomials are incredibly useful mathematical tools as they are simply defined, can be computed very quickly on computer systems and can represent a variety of functions. They can also be integrated easily and pieced together to form spline curves that can approximate any function to any accuracy desired. In the calculus courses, it is well known that a polynomial of degree N can be constructed as follows

$$f_N(t) = \sum_{i=0}^{N} a_i t^{N-i} \tag{9}$$

It is interesting to investigate the capability of the last equation, Eq. (9), from a function approximation point of view. Herein, we will prove that Eq. (9) has the universal approximation capability. In the following, we suppose that the input universe of discourse T is a convex set in $\Re$. First, we need the following useful theorem. In this theorem, the variable "t" means time and the dimension of the compact set "T" is one.

Stone–Weierstrass theorem [17]
Let o be a set of real continuous functions on a convex set T. If

1. The set o is algebra, that is the set o is closed under multiplication, addition and scalar multiplication;
2. The set o separates points of T, that is,

$$\forall\, t_1, \quad t_2 \in T, \quad t_1 \neq t_2, \quad \exists f_N(t) \in o : f_N(t_1) \neq f_N(t_2) \tag{10}$$

3. The set o vanishes at no point of T, that is,

$$\forall t \in T, \quad \exists f_N(t) \in o : f_N(t) \neq 0 \tag{11}$$

Then, for any real continuous function $f(t)$ on T and arbitrary $\varepsilon > 0$, there exists a function $f_N(t)$ in o such that

$$\underset{t \in T}{Sup} \, |f_N(t) - f(t)| < \varepsilon \tag{12}$$

Proposition 1 (**Universal approximation theorem).** *Let $f(t)$ be a continuous real function on the convex set T in $\Re$. Then, for each arbitrary $\varepsilon > 0$, there exists a function in the form of*

$$f_N(t) = \sum_{i=0}^{N} a_i t^{N-i} \tag{13}$$

such that

$$\underset{t \in T}{Sup} \left| \sum_{i=0}^{N} a_i t^{N-i} - f(t) \right| < \varepsilon \tag{14}$$

Proof of Proposition 1. Let o be a set of continuous function on T. Now, suppose $f_{N,1}(t)$ and $f_{N,2}(t)$ are given as

$$f_{N,1}(t) = \sum_{i=0}^{N} a_i t^{N-i}$$

$$f_{N,2}(t) = \sum_{j=0}^{N} \bar{a}_j t^{N-j} \tag{15}$$

https://doi.org/10.1017/S0263574720001009 Published online by Cambridge University Press

we have

$$f_{N,1}(t) + f_{N,2}(t) = \sum_{i=0}^{N} a_i t^{N-i} + \sum_{j=0}^{N} \bar{a}_j t^{N-j} \tag{16}$$

$$f_{N,1}(t).f_{N,2}(t) = \left(\sum_{i=0}^{N} a_i t^{N-i}\right).\left(\sum_{j=0}^{N} \bar{a}_j t^{N-j}\right) \tag{17}$$

Hence, $f_{N,1}(t) + f_{N,2}(t) \in o$ and $f_{N,1}(t).f_{N,2}(t) \in o$. Furthermore, for any arbitrary $\varsigma \in \Re$, we can get

$$\varsigma.f_N(t) = \sum_{i=0}^{N} \varsigma a_i t^{N-i} \tag{18}$$

which is also in the form of (9). So, according to (16) to (18), we can conclude that o is an algebra. Therefore, the first condition of the Stone–Weierstrass theorem is satisfied for o. Now, we show that o separates various points on T. Choose the parameters of $f_N(t)$ in (9) as $N = 1$. Since $t_1 \neq t_2$, then $a_0 + a_1 t_1 \neq a_0 + a_1 t_2$, which can be simplified to $t_1 \neq t_2$. Therefore, the second condition is also verified. To show that o vanishes at no point of T, we simply observe that any function in the form of (9) with $a_N \neq 0$, and $a_i = 0$ for i = 0, 1, .., N − 1 has the property of

$$\forall t \in T, \quad f_N(t) \neq 0 \tag{19}$$

Hence, o vanishes at no point of T. Thus, the three conditions of the Stone–Weierstrass theorem are satisfied. Therefore, the result follows by Stone–Weierstrass theorem.

5. Control Design

Based on the aforementioned discussion, a polynomial-based adaptive impedance controller is developed for robotic systems. The controller will be designed in the following order. At first, fictitious control law I_d is designed for I, which is not actual control input of the manipulator. Next, the actual control signal $u(t)$ is constructed in (2) to ensure convergence of I to I_d which results in convergence of h to desired trajectory h_t.

5.1. The output-tracking control loop

As a preliminary to the control design, let us define the actuator current tracking error as $e_I = (I - I_d) \in \Re^n$. Therefore, the robot dynamic (6) can be rewritten as

$$\ddot{h} = J(q)^{-T} H e_I + J(q)^{-T} H I_d - F_{ext} + \Xi(t) \tag{20}$$

Where $\Xi(t) \in \Re^n$ represents the lumped uncertainty denoted by

$$\Xi(t) = (I_n - M(h))\ddot{h} - C'(h, \dot{h})\dot{h} - G(h) \tag{21}$$

and I_n denotes the identity matrix. Before we proceed with the details of controller derivation, consider the three following assumptions.

Assumption 1. *The manipulator is operating away from any singularity. In other words, the robot moves in the space in which $J(q)$ is non-singular.*

Assumption 2. *The nonlinear term $\Xi(t)$ is assumed to be an unknown function, and its upper and lower bounds are also assumed to be unavailable.*

Assumption 3. *The desired joint trajectories and their time derivatives are in L_∞ spaces [33].*

As a result of Assumption 2, traditional adaptive control scheme is not applicable. Under these circumstances, a PD type control law supported by an auxiliary control input $\upsilon(t) \in \Re^n$ is proposed as

$$I_d(t) = H^{-1} J(q)^T \left(F_{ext} + \ddot{h}_t - K_p \tilde{h} - K_d \dot{\tilde{h}} + K_p \upsilon(t)\right) \tag{22}$$

https://doi.org/10.1017/S0263574720001009 Published online by Cambridge University Press

where $K_p \in \Re^{n\times n}$ and $K_d \in \Re^{n\times n}$ are positive proportional and derivative gain matrices, respectively, and $\tilde{h} = h - h_t$. Substituting (22) into (20) leads to

$$\dot{x}(t) = Ax(t) + B(J(q)^{-T}He_I + K_p\upsilon(t) + \Xi(t)) \tag{23}$$

where

$$A = \begin{bmatrix} 0_n & I_n \\ -K_p & -K_d \end{bmatrix} \in \Re^{2n\times 2n}, \quad B = \begin{bmatrix} 0_n \\ I_n \end{bmatrix} \in \Re^{2n\times n}, \quad x(t) = \begin{bmatrix} \tilde{h}^T & \dot{\tilde{h}}^T \end{bmatrix}^T \in \Re^{2n}$$

Now, the control problem can be stated as designing a control input $\upsilon(t)$ such that, $x(t)$ converges to zero or at least it is bounded by a constant. With this in mind, the universal approximation theorem will be used to represent $\Xi(t)$ as linear combinations of basis functions as

$$\Xi(t) = W_\Xi^T Z_\Xi + \varepsilon_\Xi \tag{24}$$

where $W_\Xi \in \Re^{(nN_1+n)\times n}$ is a block diagonal constant matrix, N_1 is the degree of polynomial function, $Z_\Xi \in \Re^{(nN_1+n)}$ is the vector of basis functions which will be defined later and $\varepsilon_\Xi \in \Re^n$ is the approximation error of $\Xi(t)$. This approximation opens the opportunity to design the control law $\upsilon(t)$ based on compensation of the perturbation present in the plant. Making use of the polynomial-based uncertainty estimator, we propose

$$\upsilon(t) = -K_p^{-1}\hat{W}_\Xi^T Z_\Xi \tag{25}$$

where

$$\hat{W}_\Xi^T = \begin{bmatrix} \hat{W}_{\Xi,1}^T & 0 & 0 & \cdots & 0 & 0 \\ 0 & \hat{W}_{\Xi,2}^T & 0 & \cdots & 0 & 0 \\ \vdots & 0 & \hat{W}_{\Xi,3}^T & \vdots & \vdots & \vdots \\ \vdots & \vdots & \cdots & \cdots & \hat{W}_{\Xi,n-1}^T & 0 \\ 0 & 0 & \cdots & \cdots & 0 & \hat{W}_{\Xi,n}^T \end{bmatrix} \in \Re^{n\times(nN_1+n)} \tag{26}$$

$$Z_\Xi = [\underbrace{y^T \cdots y^T}_{n}]^T \in \Re^{nN_1+n} \tag{27}$$

With $\hat{W}_{\Xi,i} = \begin{bmatrix} \hat{a}_{i,N_1} & \hat{a}_{i,N_1-1} & \ldots & \hat{a}_{i,0} \end{bmatrix}^T \in \Re^{N_1+1}$, $i = 1, 2, \ldots,$ n and $y = \begin{bmatrix} 1, & t, & \ldots & t^{N_1} \end{bmatrix}^T \in \Re^{N_1+1}$. Notice that the set of functions $\{1, t, t^2, \ldots t^{N_1}\}$ form a basis for function for this vector space. Now, substituting (24) and (25) into (23), we obtain the output-tracking loop dynamics as

$$\dot{x}(t) = Ax(t) + B(J(q)^{-T}He_I + \tilde{W}_\Xi^T Z_\Xi + \varepsilon_\Xi) \tag{28}$$

where $\tilde{W}_\Xi = W_\Xi - \hat{W}_\Xi$ is the parametric estimation error.

5.2. The current tracking control loop

Here, the control objective is to design a control input $u(t)$ to realize the perfect motor current vector in (22) with the aim of reducing the error signal e_I as small as possible. It returns to this fact that, a constant-bounded disturbance will not destroy the stability result under robust control I_d which is a result of uniform ultimate boundedness of the tracking error using the Lyapunov-based theory of guaranteed stability of uncertain systems [34]. With this in mind, we propose the following control input

$$u(t) = \hat{f} - K_c e_I \tag{29}$$

where $\hat{f}$ is the estimate of $f = L\dot{I}_d + RI + K_b\dot{q}$ and $K_c \in \Re^{n\times n}$ is a constant diagonal matrix of desired error dynamics. The current tracking loop dynamics with the controller (29) and motor (2)

https://doi.org/10.1017/S0263574720001009 Published online by Cambridge University Press

can then be represented in the form of

$$L\dot{e}_I + K_c e_I = \hat{f} - f \tag{30}$$

Following the same procedure as previous section, a polynomial-based uncertainty estimator will be used to represent the uncertainty term $\hat{f}$ as

$$\hat{f} = \left[\, \hat{f}_1(t)\ \ \hat{f}_2(t)\ \ldots\ \hat{f}_n(t) \,\right]^T \in \Re^n \tag{31}$$

in which

$$\hat{f}_i(t) = \sum_{j=0}^{N_2} \hat{b}_{i,j} t^{N_2 - j}, \quad i = 1, 2, ..., \text{n} \tag{32}$$

with f_i denoting the i-th row of the lumped uncertainty f. Equation (31) can be represented as follows

$$\hat{f} = \left[\sum_{j=0}^{N_2} \hat{b}_{1,j} t^{N_2 - j} \sum_{j=0}^{N_2} \hat{b}_{2,j} t^{N_2 - j} \ldots \sum_{j=0}^{N_2} \hat{b}_{n,j} t^{N_2 - j} \right]^T \tag{33}$$

One can easily represent (33) as

$$\hat{f} = \hat{W}_f^T Z_f \tag{34}$$

where $\hat{W}_f^T$ and Z_f are expressed as

$$\hat{W}_f^T = \begin{bmatrix} \hat{W}_{f,1}^T & 0 & 0 & \cdots & 0 & 0 \\ 0 & \hat{W}_{f,2}^T & 0 & \cdots & 0 & 0 \\ \vdots & 0 & \hat{W}_{f,3}^T & \vdots & \vdots & \vdots \\ \vdots & \vdots & \cdots & \cdots & \hat{W}_{f,n-1}^T & 0 \\ 0 & 0 & \cdots & \cdots & 0 & \hat{W}_{f,n}^T \end{bmatrix} \in \Re^{n \times (nN_2 + n)} \tag{35}$$

$$Z_f = [\underbrace{y^T \cdots y^T}_{n}]^T \in \Re^{nN_2 + n} \tag{36}$$

with $\hat{W}_{f,i} = \left[\, \hat{b}_{i,N_2}\ \hat{b}_{i,N_2-1}\ \ldots\ \hat{b}_{i,0} \,\right]^T \in \Re^{N_2+1}$, $i = 1, 2, ..., \text{n}$ and $y = \left[\, 1,\ t,\ ...,\ t^{N_2} \,\right]^T \in \Re^{N_2+1}$. Suppose that f can be modeled as

$$f = W_f^T Z_f + \varepsilon_f \tag{37}$$

where $\varepsilon_f \in \Re^n$ is the bounded approximation error and matrix $W_f \in \Re^{(nN_2+n)\times n}$ is a block diagonal constant matrix. Define the parameter error vector as $\tilde{W}_f = W_f - \hat{W}_f$. Now, Eq. (30) can be represented by

$$L\dot{e}_I + K_c e_I = -\tilde{W}_f^T Z_f + \varepsilon_f \tag{38}$$

which is a stable linear time invariant system driven by the parameter error as well as the approximation error.

5.3. Stability analysis

To carry out the stability analysis of the closed-loop system formed by the robot dynamic model (1), (2), together with the controller (22) and (29), the following Lyapunov function candidate is proposed:

$$V(x, e_I, \tilde{W}_\Xi, \tilde{W}_f) = \frac{1}{2}[x^T P x + e_I^T L e_I + Tr(\tilde{W}_\Xi^T \Gamma_\Xi \tilde{W}_\Xi) + Tr(\tilde{W}_f^T \Gamma_f \tilde{W}_f)] \tag{39}$$

https://doi.org/10.1017/S0263574720001009 Published online by Cambridge University Press

Differentiating (39) with respect to time and using (28) and (38) yield in

$$\begin{aligned}\dot{V}(x, e_I, \tilde{W}_\Xi, \tilde{W}_f) = &\frac{1}{2}x^T(A^T P + PA)x - e_I^T K_c e_I + x^T PBJ(q)^{-T} He_I \\ &+ x^T PB\varepsilon_\Xi + e_I^T \varepsilon_f + x^T PB\tilde{W}_\Xi^T Z_\Xi - e_I^T \tilde{W}_f^T Z_f \\ &- Tr(\tilde{W}_\Xi^T \Gamma_\Xi \hat{W}_\Xi) - Tr(\tilde{W}_f^T \Gamma_f \hat{W}_f)\end{aligned} \tag{40}$$

where $\Gamma_\Xi \in \Re^{(nN_1+n)\times(nN_1+n)}$ and $\Gamma_f \in \Re^{(nN_2+n)\times(nN_2+n)}$ are all positive definite matrices. Since A is Hurwitz, one can arbitrarily choose a positive definite matrix Q and let $P \in \Re^{2n\times 2n}$ be the unique symmetric positive definite matrix that satisfies the Lyapunov equation

$$A^T P + PA = -Q \tag{41}$$

Thus, substituting (41) into (40) we have

$$\begin{aligned}\dot{V}(x, e_I, \tilde{W}_\Xi, \tilde{W}_f) = &-\frac{1}{2}x^T Qx - e_I^T K_c e_I + x^T PBJ(q)^{-T} He_I \\ &+ x^T PB\varepsilon_\Xi + e_I^T \varepsilon_f - Tr(\tilde{W}_\Xi^T(\Gamma_\Xi \dot{\hat{W}}_\Xi - Z_\Xi x^T PB)) \\ &- Tr(\tilde{W}_f^T(\Gamma_f \dot{\hat{W}}_f + Z_f e_I^T))\end{aligned} \tag{42}$$

By selecting the update laws as

$$\begin{aligned}\dot{\hat{W}}_\Xi &= \Gamma_\Xi^{-1}(Z_\Xi x^T PB - \sigma_\Xi \hat{W}_\Xi) \\ \dot{\hat{W}}_f &= -\Gamma_f^{-1}(Z_f e_I^T + \sigma_f \hat{W}_f)\end{aligned} \tag{43}$$

where $\sigma_{(\bullet)}$ are positive numbers, (42) is simplified to

$$\begin{aligned}\dot{V}(x, e_I, \tilde{W}_\Xi, \tilde{W}_f) = &-\begin{bmatrix} x^T & e_I^T \end{bmatrix} \Lambda \begin{bmatrix} x \\ e_I \end{bmatrix} + \begin{bmatrix} x^T & e_I^T \end{bmatrix} P' \begin{bmatrix} \varepsilon_\Xi \\ \varepsilon_f \end{bmatrix} \\ &+ \sigma_\Xi Tr(\tilde{W}_\Xi^T \hat{W}_\Xi) + \sigma_f Tr(\tilde{W}_f^T \hat{W}_f)\end{aligned} \tag{44}$$

where

$$\Lambda = \begin{bmatrix} \frac{1}{2}Q & -\frac{1}{2}PBJ(q)^{-T}H \\ -\frac{1}{2}(PBJ(q)^{-T}H)^T & K_c \end{bmatrix}$$

is a positive definite matrix by proper selection of K_c and Q, and $P' = \begin{bmatrix} PB & 0_{2n\times n} \\ 0_n & I_n \end{bmatrix} \in \Re^{3n\times 2n}$.

Result 1. *Suppose a sufficient number of basis functions are used and the approximation error can be ignored, then it is not necessary to include the σ-modification terms in* (43)*. Hence,* (44) *can be reduced to*

$$\dot{V}(x, e_I, \tilde{W}_\Xi, \tilde{W}_f) \le -\begin{bmatrix} x^T & e_I^T \end{bmatrix} \Lambda \begin{bmatrix} x \\ e_I \end{bmatrix} \le 0 \tag{45}$$

and asymptotic convergence of x and e_I can be concluded using the Barbalat's Lemma.

Result 2. *Owing to the existence of ε_Ξ and ε_I in* (44)*, it is very easy to prove the following inequalities hold*

https://doi.org/10.1017/S0263574720001009 Published online by Cambridge University Press

$$
\begin{aligned}
&-\left[x^T\ e_I^T\right]\Lambda\begin{bmatrix}x\\ e_I\end{bmatrix}+\left[x^T\ e_I^T\right]P'\begin{bmatrix}\varepsilon_\Xi\\ \varepsilon_f\end{bmatrix}\\
&\qquad\le-\frac{1}{2}\lambda_{\min}(\Lambda)\left\|\begin{bmatrix}x\\ e_I\end{bmatrix}\right\|^2+\frac{\sigma_{\max}^2(P')}{2\lambda_{\min}(\Lambda)}\left\|\begin{bmatrix}\varepsilon_\Xi\\ \varepsilon_f\end{bmatrix}\right\|^2,\\
&Tr(\tilde{W}_{(\bullet)}^T\hat{W}_{(\bullet)})\le\frac{1}{2}Tr(W_{(\bullet)}^TW_{(\bullet)})-\frac{1}{2}Tr(\tilde{W}_{(\bullet)}^T\tilde{W}_{(\bullet)})
\end{aligned}
\tag{46}
$$

where $\sigma_{\max}(P')$ *denotes maximum singular value of matrix* P'*. Together with this relationship*

$$
\begin{aligned}
V(x,e_I,\tilde{W}_\Xi,\tilde{W}_f)\le\frac{1}{2}\Bigg[&\lambda_{\max}(\Phi)\left\|\begin{bmatrix}x\\ e_I\end{bmatrix}\right\|^2+\lambda_{\max}(\Gamma_\Xi)Tr(\tilde{W}_\Xi^T\tilde{W}_\Xi)\\
&+\lambda_{\max}(\Gamma_f)Tr(\tilde{W}_f^T\tilde{W}_f)\Bigg]
\end{aligned}
\tag{47}
$$

where $\Phi=\begin{bmatrix}P & 0\\ 0 & L\end{bmatrix}$*, we may write* (44) *in the form of*

$$
\begin{aligned}
\dot{V}(x,e_I,\tilde{W}_\Xi,\tilde{W}_f)\le&-\mu V+\frac{1}{2}\left(\mu\lambda_{\max}(\Phi)-\lambda_{\min}(\Lambda)\right)\left\|\begin{bmatrix}x\\ e_I\end{bmatrix}\right\|^2\\
&+\frac{1}{2}(\mu\lambda_{\max}(\Gamma_\Xi)-\sigma_\Xi)Tr(\tilde{W}_\Xi^T\tilde{W}_\Xi)\\
&+\frac{1}{2}(\mu\lambda_{\max}(\Gamma_f)-\sigma_f)Tr(\tilde{W}_f^T\tilde{W}_f)\\
&+\frac{1}{2}\left[\frac{\sigma_{\max}^2(P')}{\lambda_{\min}(\Lambda)}\left\|\begin{bmatrix}\varepsilon_\Xi\\ \varepsilon_f\end{bmatrix}\right\|^2+\sigma_\Xi Tr(W_\Xi^TW_\Xi)+\sigma_f Tr(W_f^TW_f)\right]
\end{aligned}
\tag{48}
$$

By selecting $\mu\le\min\left\{\frac{\lambda_{\min}(\Lambda)}{\lambda_{\max}(\Phi)},\frac{\sigma_\Xi}{\lambda_{\max}(\Gamma_\Xi)},\frac{\sigma_f}{\lambda_{\max}(\Gamma_f)}\right\}$*, then* (48) *can be further derived as*

$$
\begin{aligned}
\dot{V}(x,e_I,\tilde{W}_\Xi,\tilde{W}_f)\le-\mu V+\frac{1}{2}\Bigg[&\frac{\sigma_{\max}^2(P')}{\lambda_{\min}(\Lambda)}\left\|\begin{bmatrix}\varepsilon_\Xi\\ \varepsilon_f\end{bmatrix}\right\|^2+\sigma_\Xi Tr(W_\Xi^TW_\Xi)\\
&+\sigma_f Tr(W_f^TW_f)\Bigg]
\end{aligned}
\tag{49}
$$

This implies that $\dot{V}<0$ *whenever*

$$
V>\frac{\sigma_{\max}^2(P')}{2\mu\lambda_{\min}(\Lambda)}\sup_{t_0<\tau<t}\left\|\begin{bmatrix}\varepsilon_\Xi(\tau)\\ \varepsilon_f(\tau)\end{bmatrix}\right\|^2+\frac{1}{2\mu}[\sigma_\Xi Tr(W_\Xi^TW_\Xi)+\sigma_f Tr(W_f^TW_f)]
\tag{50}
$$

Hence, we have proved that $(x,e_I,\tilde{W}_\Xi,\tilde{W}_f)$ *are UUB.*

Because x is bounded, boundedness of $x(t)=\left[\tilde{h}^T\ \dot{\tilde{h}}^T\right]^T$ can be obtained, whereas h_t and $\dot{h}_t$ are bounded. Since the Jacobian matrix is non-singular, boundedness of $\dot{q}=J(q)^{-1}\dot{h}$ can also be obtained, whereas $\dot{h}$ is bounded. In addition, $q=\int_0^t J^{-1}(q)\dot{h}\mathrm{d}t+q(0)$ is also bounded, for finite operational times. Therefore, the robotic system will be stabilized with UUB performance under the proposed design.

5.4. Performance evaluation

The stability analysis presented in the previous section only demonstrates boundedness of $(x,e_I,\tilde{W}_\Xi,\tilde{W}_f)$, but in practical applications, the transient performance is also of great importance. For further development, we may solve the differential inequality in (49) to calculate the upper bound for $V(t)$.

https://doi.org/10.1017/S0263574720001009 Published online by Cambridge University Press

$$V(t) \le e^{-\mu(t-t_0)}V(t_0) + \frac{\sigma_{\max}^2(P')}{2\mu\lambda_{\min}(\Lambda)} \sup_{t_0<\tau<t} \left\| \begin{bmatrix} \varepsilon_\Xi(\tau) \\ \varepsilon_f(\tau) \end{bmatrix} \right\|^2 + \frac{1}{2\mu}[\sigma_\Xi Tr(W_\Xi^T W_\Xi) + \sigma_f Tr(W_f^T W_f)] \tag{51}$$

Consider the lower bound of $V(t)$ in (39) as

$$V(x, e_I, \tilde{W}_\Xi, \tilde{W}_f) \ge \frac{1}{2}\lambda_{\min}(\Phi) \left\| \begin{bmatrix} x \\ e_I \end{bmatrix} \right\|^2 + \frac{1}{2}[\lambda_{\min}(\Gamma_\Xi) Tr(\tilde{W}_\Xi^T \tilde{W}_\Xi) + \lambda_{\min}(\Gamma_f) Tr(\tilde{W}_f^T \tilde{W}_f)] \tag{52}$$

This implies that $\left\| \begin{bmatrix} x \\ e_I \end{bmatrix} \right\| \le \sqrt{\frac{2V(x, e_I, \tilde{W}_\Xi, \tilde{W}_f)}{\lambda_{\min}(\Phi)}}$. Together with (51), we may compute the bound as

$$\left\| \begin{bmatrix} x \\ e_I \end{bmatrix} \right\| \le \sqrt{\frac{2V(t_0)}{\lambda_{\min}(\Phi)}} e^{\frac{-\mu(t-t_0)}{2}} + \sqrt{\frac{\sigma_{\max}^2(P')}{\mu\lambda_{\min}(\Phi)\lambda_{\min}(\Lambda)}} \sup_{t_0<\tau<t} \left\| \begin{bmatrix} \varepsilon_\Xi(\tau) \\ \varepsilon_f(\tau) \end{bmatrix} \right\| + \frac{1}{\sqrt{\mu\lambda_{\min}(\Phi)}}[\sigma_\Xi Tr(W_\Xi^T W_\Xi) + \sigma_f Tr(W_f^T W_f)]^{\frac{1}{2}} \tag{53}$$

This proves that the time history of $\left\| \begin{bmatrix} x \\ e_I \end{bmatrix} \right\|$ is bounded by an exponential function plus some constants. This also implies that by adjusting controller parameters, we may improve output error convergence rate. As a consequence,

$$\lim_{t\to\infty} \left\| \begin{bmatrix} x \\ e_I \end{bmatrix} \right\| \le \sqrt{\frac{\sigma_{\max}^2(P')}{\mu\lambda_{\min}(\Phi)\lambda_{\min}(\Lambda)}} \sup_{t_0<\tau<t} \left\| \begin{bmatrix} \varepsilon_\Xi(\tau) \\ \varepsilon_f(\tau) \end{bmatrix} \right\| + \frac{1}{\sqrt{\mu\lambda_{\min}(\Phi)}}[\sigma_\Xi Tr(W_\Xi^T W_\Xi) + \sigma_f Tr(W_f^T W_f)]^{\frac{1}{2}} \tag{54}$$

Considering the Frobenius norm definition, $\left(\left\| \tilde{W}_{(\bullet)} \right\|_F^2 = Tr(\tilde{W}_{(\bullet)}^T \tilde{W}_{(\bullet)}) \right)$, one can also obtain the following bounds for the weighting vector $\tilde{W}_\Xi$ and $\tilde{W}_f$, respectively.

$$\lim_{t\to\infty} \left\| \tilde{W}_\Xi \right\|_F \le \sqrt{\frac{\sigma_{\max}^2(P')}{\mu\lambda_{\min}(\Gamma_\Xi)\lambda_{\min}(\Lambda)}} \sup_{t_0<\tau<t} \left\| \begin{bmatrix} \varepsilon_\Xi(\tau) \\ \varepsilon_f(\tau) \end{bmatrix} \right\| + \frac{1}{\sqrt{\mu\lambda_{\min}(\Gamma_\Xi)}}[\sigma_\Xi Tr(W_\Xi^T W_\Xi) + \sigma_f Tr(W_f^T W_f)]^{\frac{1}{2}} \tag{55}$$

$$\lim_{t\to\infty} \left\| \tilde{W}_f \right\|_F \le \sqrt{\frac{\sigma_{\max}^2(P')}{\mu\lambda_{\min}(\Gamma_f)\lambda_{\min}(\Lambda)}} \sup_{t_0<\tau<t} \left\| \begin{bmatrix} \varepsilon_\Xi(\tau) \\ \varepsilon_f(\tau) \end{bmatrix} \right\| + \frac{1}{\sqrt{\mu\lambda_{\min}(\Gamma_f)}}[\sigma_\Xi Tr(W_\Xi^T W_\Xi) + \sigma_f Tr(W_f^T W_f)]^{\frac{1}{2}} \tag{56}$$

The transient performance analysis is then completed.

6. Simulation Results

In this section, we present simulation results for the proposed control scheme. The simulation task is carried out based on a two DOF planer robot including the actuator dynamics. The dynamic model of the robot system can be described in the form of Eq. (1) as [35]

$$D(q) = \begin{bmatrix} m_1 l_{c1}^2 + I_1 + m_2(l_1^2 + l_{c2}^2 + 2l_1 l_{c2}\cos(q_2)) + I_2 & m_2 l_{c2}^2 + m_2 l_1 l_{c2}\cos(q_2) + I_2 \\ m_2 l_{c2}^2 + m_2 l_1 l_{c2}\cos(q_2) + I_2 & m_2 l_{c2}^2 + I_2 \end{bmatrix}$$

https://doi.org/10.1017/S0263574720001009 Published online by Cambridge University Press

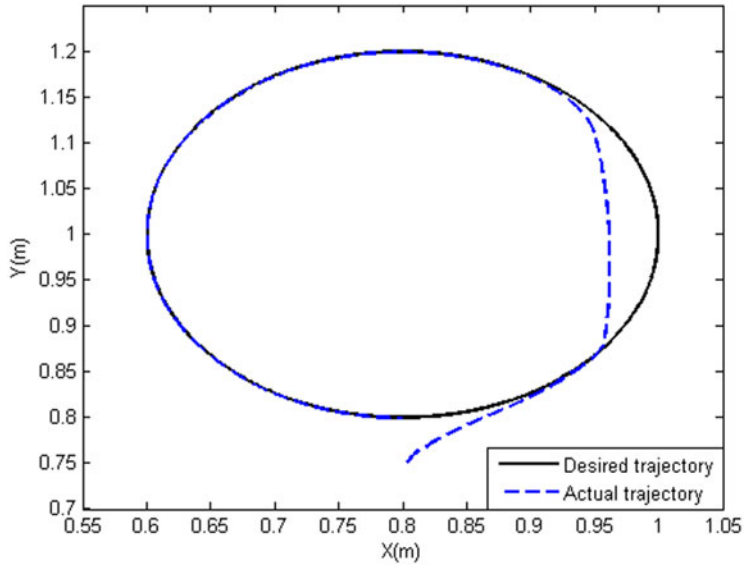


Fig. 1. Tracking performance of endpoint in the task space.

$$C(q,\dot{q})\dot{q} = \begin{bmatrix} -2m_2 l_1 l_{c2} \sin(q_2)(\dot{q}_1\dot{q}_2 + 0.5\dot{q}_2^2) \\ m_2 l_1 l_{c2} \sin(q_2)\dot{q}_1^2 \end{bmatrix}$$
$$g(q) = \begin{bmatrix} m_1 l_{c1} g \cos(q_1) + m_2 g(l_{c2}\cos(q_1+q_2) + l_1 g \cos(q_1)) \\ m_2 l_{c2} g \cos(q_1+q_2) \end{bmatrix}$$
$$J = \begin{bmatrix} -l_1 \sin(q_1) - l_2 \sin(q_1+q_2) & -l_2 \sin(q_1+q_2) \\ l_1 \cos(q_1) + l_2 \cos(q_1+q_2) & l_2 \cos(q_1+q_2) \end{bmatrix} \tag{57}$$

where q_i $(i = 1, 2)$ is the joint angle, m_i is the mass of each link, l_i is the length of each link and g is the gravity acceleration. The manipulator parameters are defined as $l_1 = l_2 = 0.75$ m, $l_{c1} = l_{c2} = 0.375$ m, $m_1 = m_2 = 0.5$ kg and $I_1 = I_2 = 0.0234$ (kgm^2). The actuator dynamic model parameters are selected as $H = \text{diag}(10, 10)$(N-m/A), $R = \text{diag}(1, 1)\Omega$, $L = \text{diag}(0.025, 0.025)$ H and $K_b = \text{diag}(1, 1)$(volt/rad/s).

Simulation 1. The endpoint starts from x(0) = [0.8 m 0.75 m 0 0]^T to track a 0.2 m radius circle centered at (0.8 m, 1 m) during 2 s. The initial condition of the target impedance states is the same as the initial value of the desired task space trajectory. We assume that the end-effector position can be obtained from a position sensor, such as vision systems, electromagnetic measurement systems, position sensitive detectors or laser trackers. The values of the parameters in $M(h)$, $H(h, \dot{h})$ and $G(h)$ are assumed to be unknown.

A vertical wall with a stiffness of $k_e = 5000\ (N/m)$ is located at $h_{x_e} = 0.95$m along the y-axis. The environment dynamic was modeled as a regular spring, that is,

$$f_{ext} = k_e(h_x - h_{x_e}) \quad \text{for } h_x \geq h_{x_e} \tag{58}$$

where f_{ext} is the force acting on the surface, k_e represents the environment dominant stiffness, h_x is the coordinate of the endpoint in the X direction and h_{x_e} denotes the location of the undeformed environment. Hence, the external force vector becomes $F_{ext} = [f_{ext}\ 0]^{\mathrm{T}}$. Parameter matrices in the target impedance are selected to be $M_t = \text{diag}(0.5,0.5)$, $B_t = \text{diag}(100,100)$, and $k_t = \text{diag}(1500, 1500)$ [31]. The controller parameters were selected as $K_p = \text{diag}(1200, 1200)$, $K_d = \text{diag}(70, 70)$ and $K_c = \text{diag}(100, 100)$.

Let us select the 3-first terms of polynomial, as the basis function for approximation of f and $\Xi(t)$. Therefore, $\hat{W}_f \in \Re^{6\times 2}$, and $\hat{W}_\Xi \in \Re^{6\times 2}$. The initial weighting matrices are also assigned to zero. The adaptive gain matrices are selected as $\Gamma_f = 10^{-4} \times I_6$ and $\Gamma_\Xi = I_6$ where $I_{(\bullet)}$ is the identity matrix. Furthermore, Q has been selected as $10^3 \times I_4$. In this step, we assume that the approximation error can be neglected and hence the σ-modification parameters are chosen as $\sigma_f = \sigma_\Xi = 0$. Under these settings, Fig. 1 represents the desired and actual trajectories of the proposed adaptive impedance

https://doi.org/10.1017/S0263574720001009 Published online by Cambridge University Press

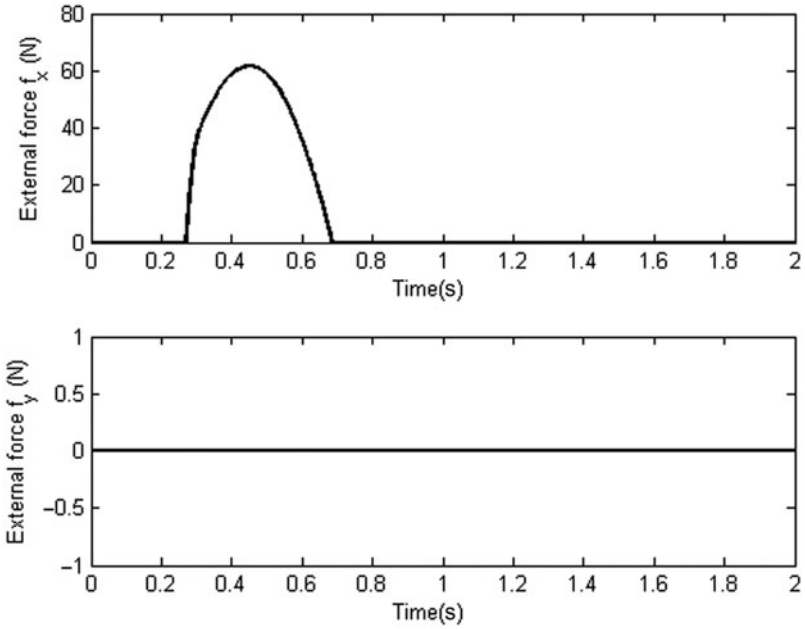


Fig. 2. External forces.

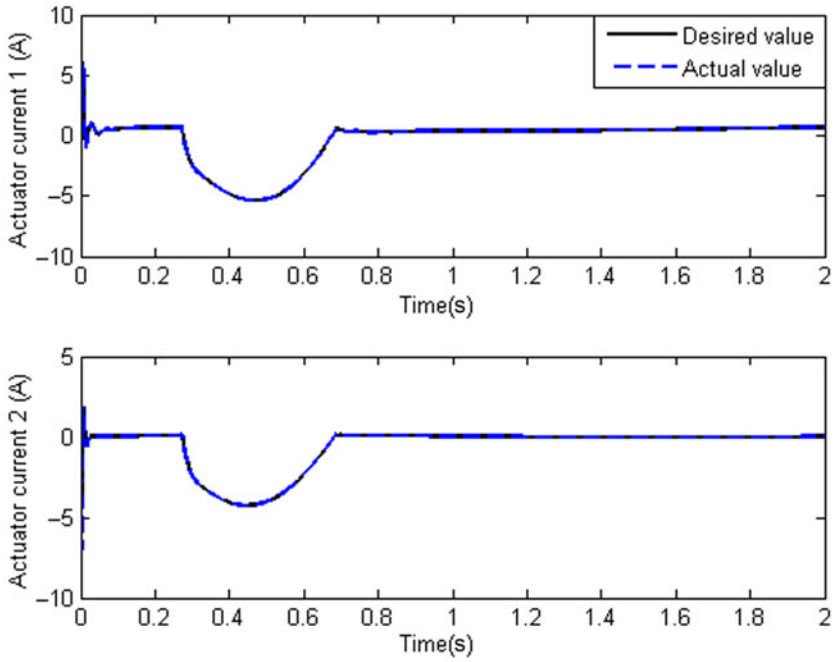


Fig. 3. Tracking in the current tracking loop.

controller in the task space. Since the surface is away from the desired initial endpoint position, different phases of operation can be observed. The robot was initially moving in free space toward the wall. Following the commanded trajectory, the manipulator comes into contact with the wall at about $t = 0.27$ s (Fig. 2), enforcing the motion of the manipulator to stop in the normal direction to the wall. Because of the constraint from the wall and the tendency of the manipulator to follow the commanded trajectory, a collision force f_{ext}, shown in Fig. 2, is generated between the manipulator and the wall. The robot end-effector slides on the surface of the wall while exerting a certain normal force during this period. The performance in the current tracking loop is very good, as shown in Fig. 3. The control voltages to the actuators are reasonable that can be verified in Fig. 4. Finally, Figs. 5 and 6 represent the function approximation performance.

https://doi.org/10.1017/S0263574720001009 Published online by Cambridge University Press

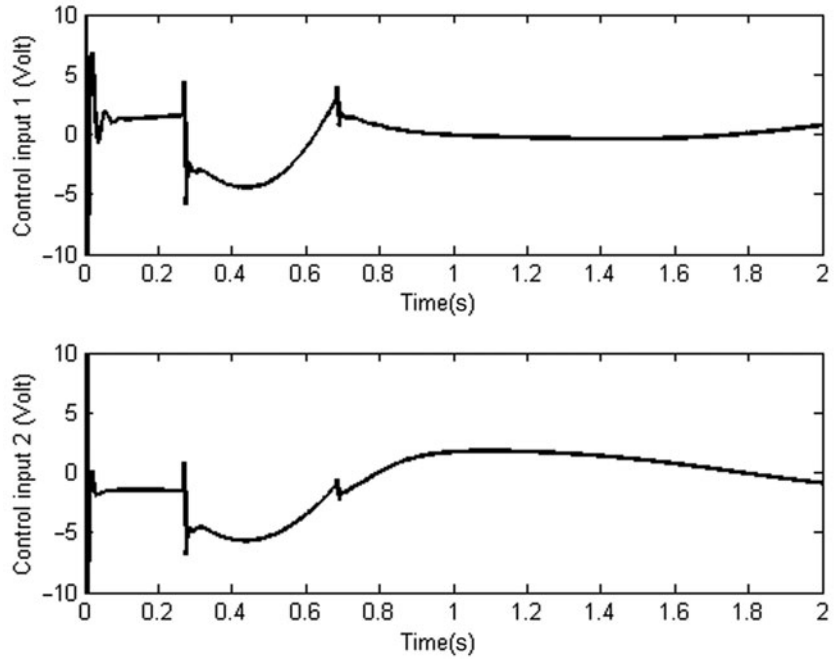


Fig. 4. Motor voltages.

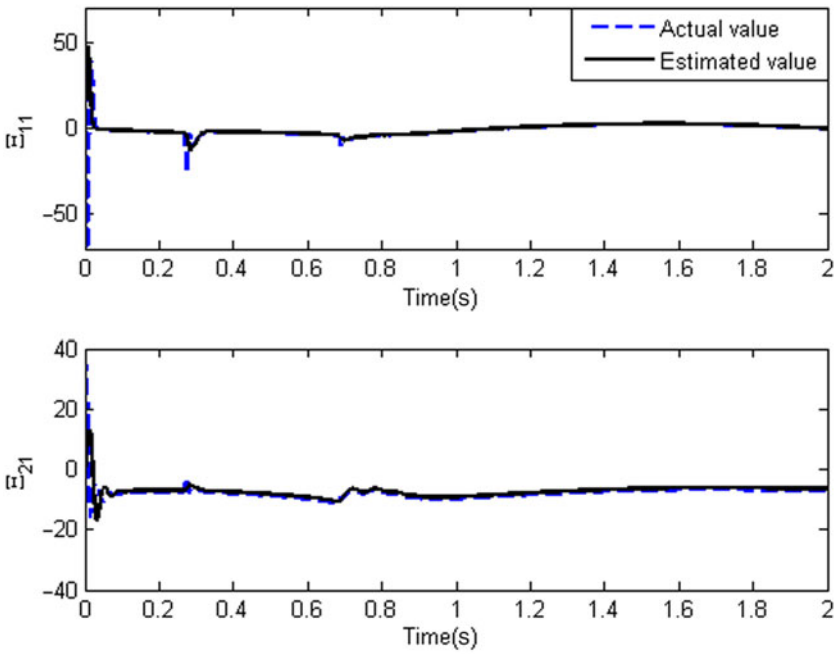


Fig. 5. Approximation of $\Xi(t)$.

For better illustration of the proposed algorithm superiority, variation of the payload and external disturbances, as the most important parameters that affect the controller performance, is considered. Toward this end, we assume that link 2 should pick up a heavy payload at $t = 0.8$ s and release it at $t = 1.5$ s during the tracking path. Since the load mass can be viewed as a part of the second link, the payload variation condition is that the mass of Δm_2 kg is added to the mass of link 2 at $t = 0.8$ s, that is, $m_2 + \Delta m_2$, and removed at $t = 1.5$ s. In this simulation, we take $\Delta m_2 = 4$ kg. The disturbance torque profile $\tau_d = [\tau_{d,1}(t)\ \tau_{d,2}(t)]^T$ in (1) for every joint is given by

https://doi.org/10.1017/S0263574720001009 Published online by Cambridge University Press

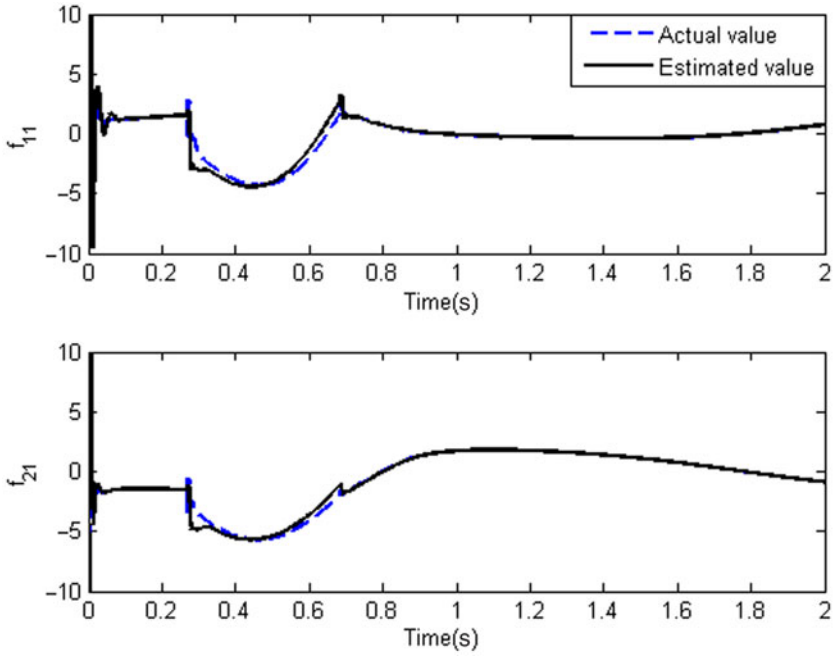


Fig. 6. Approximation of f.

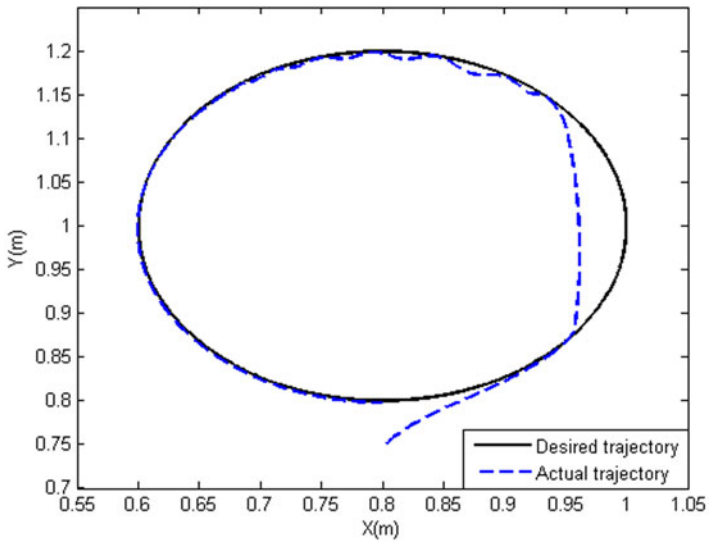


Fig. 7. Tracking performance.

$$\tau_{d,1}(t) = \begin{cases} -50t + 20 & 0 \le t \le 0.4 \\ 16.67(t - 0.4) & 0.4 \le t \le 1.6 \\ 20\cos(2.5\pi t) & 1.6 \le t \le 2 \end{cases},$$

$$\tau_{d,2}(t) = \begin{cases} 20\sin(3.33\pi t) & 0 \le t \le 0.76 \\ 0 & 0.76 \le t \le 08 \\ -20 & 0.8 \le t \le 1.2 \\ -133.33t + 179.996 & 1.2 \le t \le 1.5 \\ 40(t - 1.5) & 1.5 \le t \le 2 \end{cases} \tag{59}$$

which are strong and complex. The controller parameters are the same as before. Under these circumstances, Fig. 7 shows the tracking performances of the proposed approach subject to the

https://doi.org/10.1017/S0263574720001009 Published online by Cambridge University Press

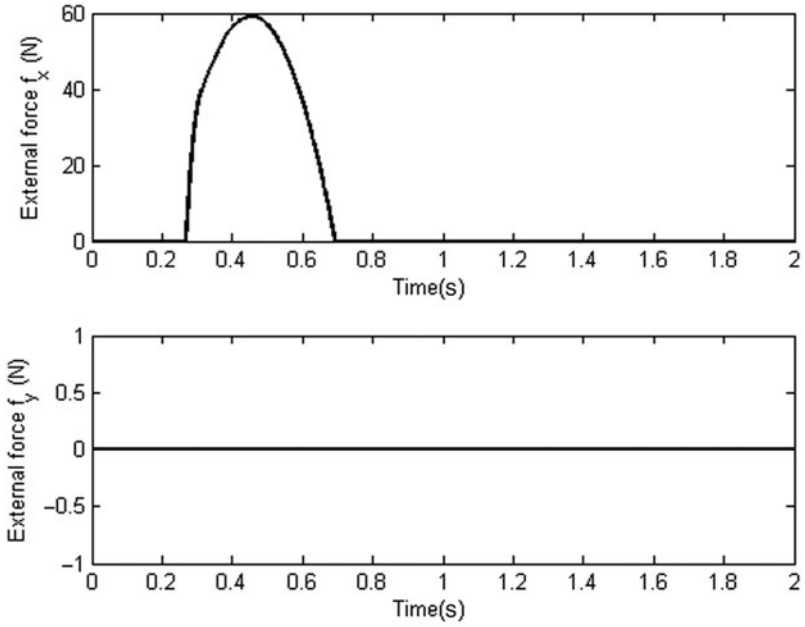


Fig. 8. External forces.

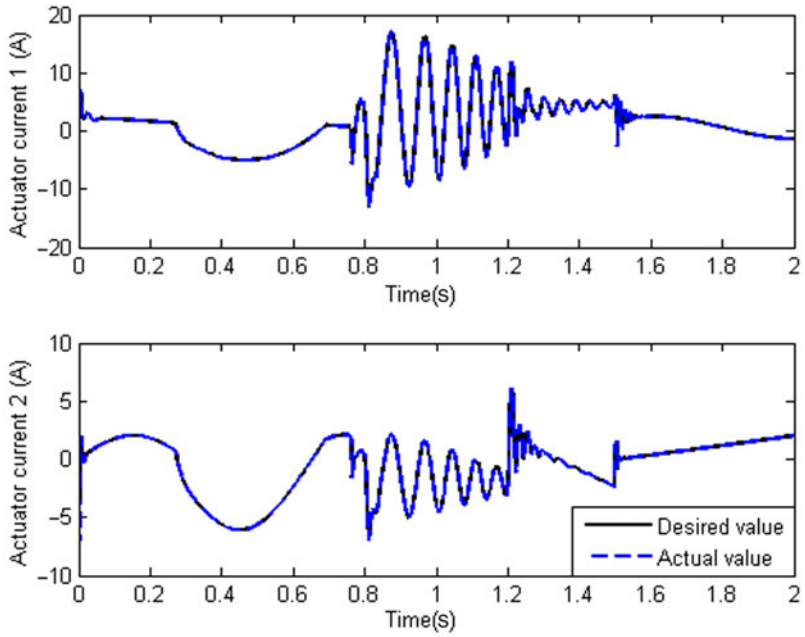


Fig. 9. Tracking in the current tracking loop.

aforementioned uncertainties. From this simulation, it is concluded that the proposed control strategy can achieve a favorable performance and represents high robustness. The external forces are presented in Fig. 8. The tracking performance in the current control loop is given in Fig. 9. The control signals are plotted in Fig. 10. As shown in this figure, motor voltages are bounded. Finally, Figs. 11 and 12 represent the function approximation performance of $\Xi(t)$ and f, respectively. To show the important role of polynomial-based uncertainty approximator, the results are simulated in the absence of $\upsilon(t)$ in the control law (22). Figure 13 shows the result of trajectory tracking in this manner.

https://doi.org/10.1017/S0263574720001009 Published online by Cambridge University Press

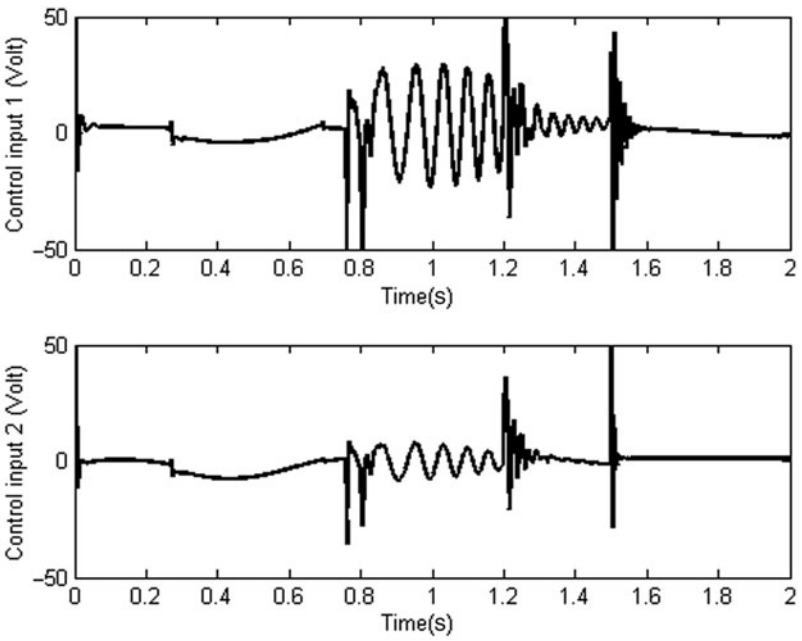


Fig. 10. Motor voltages.

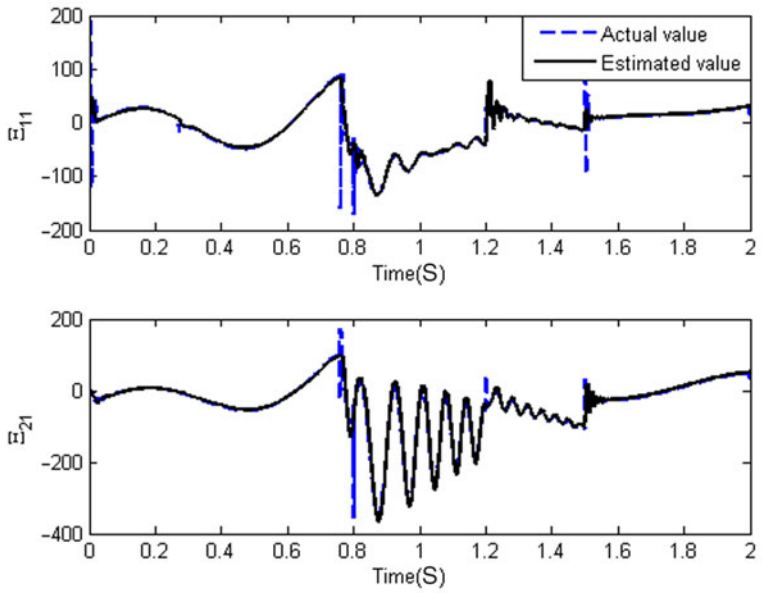


Fig. 11. Approximation of $\Xi(t)$.

Simulation 2: Highly Complex Trajectory

In order to demonstrate the capabilities of the put forward controller in certain tasks where there is a need for accurate tracking of rapid and complicated trajectories, another desired trajectory is considered. Its time equation is given in ref. [35]. Suppose that the initial manipulator configuration is $x = \left[\, 0.5\text{m}\ 0.46\text{m}\ 1.4\ -0.041 \,\right]^{\mathrm{T}}$. The above-mentioned trajectory is of immense importance, considering the fact that it involves complex and quick reactions among various dynamics of the manipulator. The controller parameters are chosen as described early on. Suppose that the stiffness of a vertical wall is $k_e = 50000\ (N/m)$ which is placed at $h_{x_e} = 0.61\ m$ along the y-axis. The results obtained from the above-described simulation can be found in Figs. 14 and 15. The tracking performance of the endpoint can be found in Fig. 14, according to which, the controller has the capability to overcome various uncertainties with negligible tracking errors. Figure 15 presents the external

https://doi.org/10.1017/S0263574720001009 Published online by Cambridge University Press

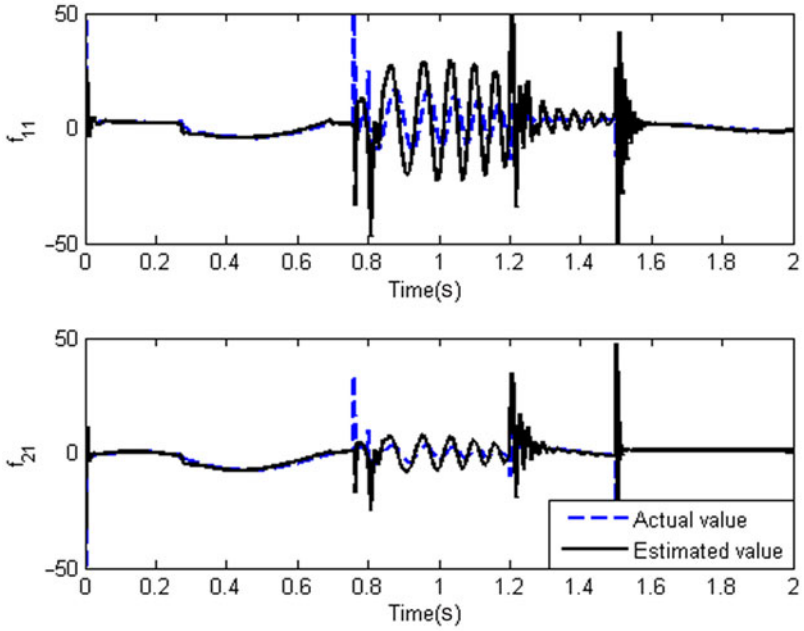


Fig. 12. Approximation of f.

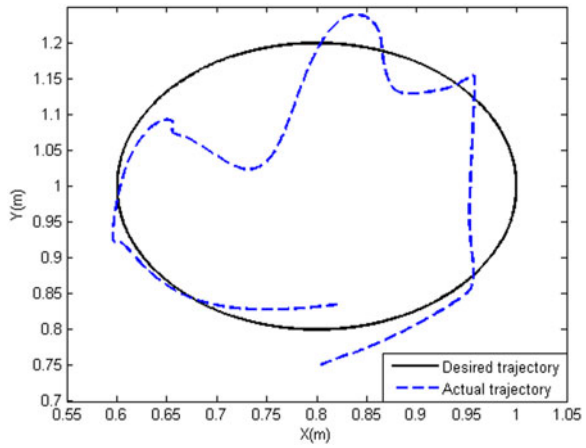


Fig. 13. Tracking performance in the absence of $\upsilon(t)$.

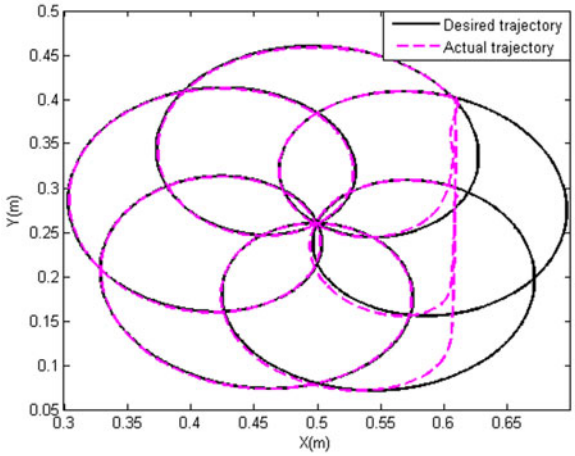


Fig. 14. Tracking performance.

https://doi.org/10.1017/S0263574720001009 Published online by Cambridge University Press

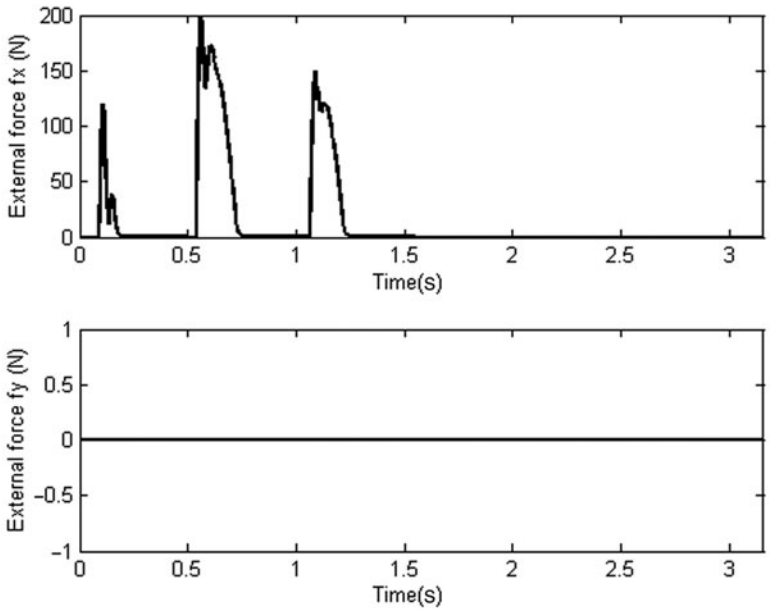


Fig. 15. External forces.

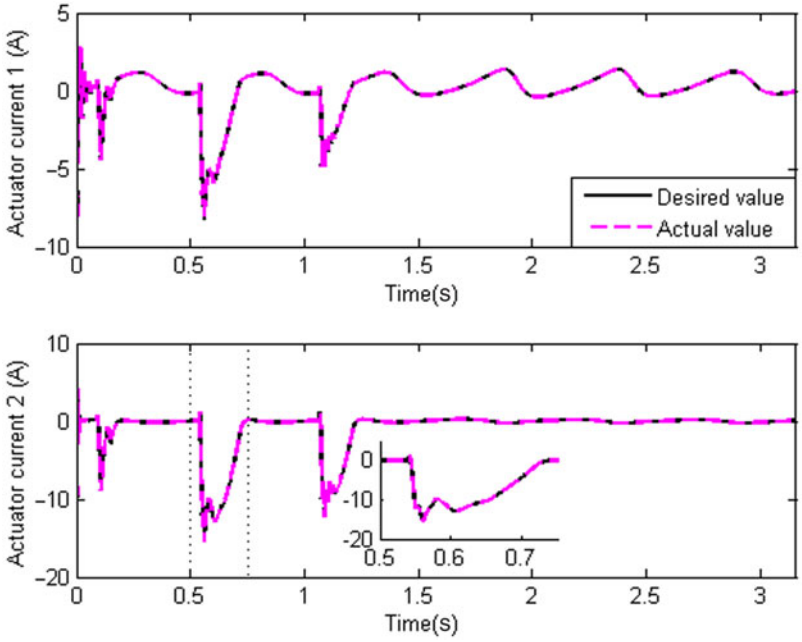


Fig. 16. The current tracking performance.

forces. As shown in this figure, when the manipulator reaches the obstacle, this force increases to high values. In Fig. 16, tracking performance of the current controller is plotted. As shown in this figure, when the external forces increase, the controller applies larger currents to cancel the undesirable influences of this force on the tracking performance. Moreover, this figure implies that in this situation, the current tracking performance is also acceptable. The control signals are plotted in Fig. 17, which are bounded. Finally, the accuracy of function approximation for the signals $\Xi(t)$ and f can be seen in Figs. 18 and 19, respectively. According to these figures, in both conditions (during the interaction and when there is no interaction), the performance of uncertainty estimation is satisfactory.

https://doi.org/10.1017/S0263574720001009 Published online by Cambridge University Press

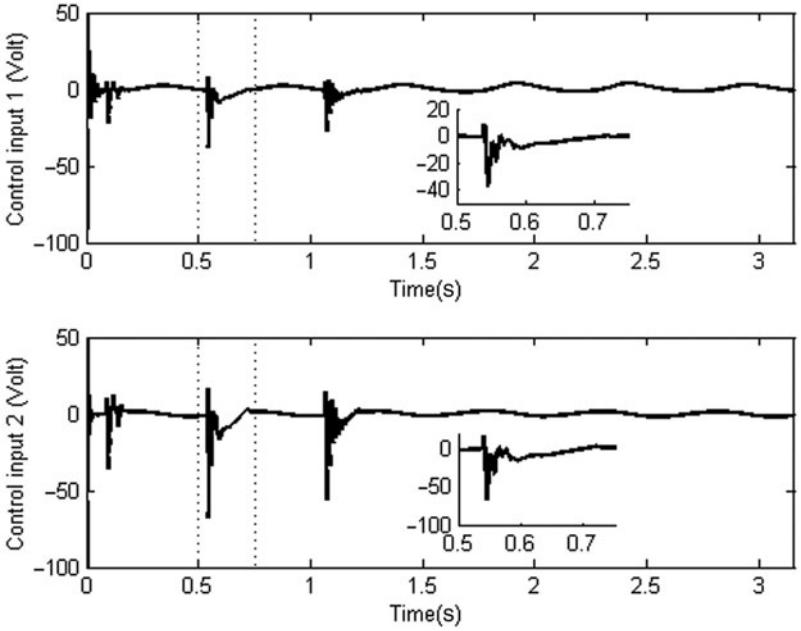


Fig. 17. Motor voltages.

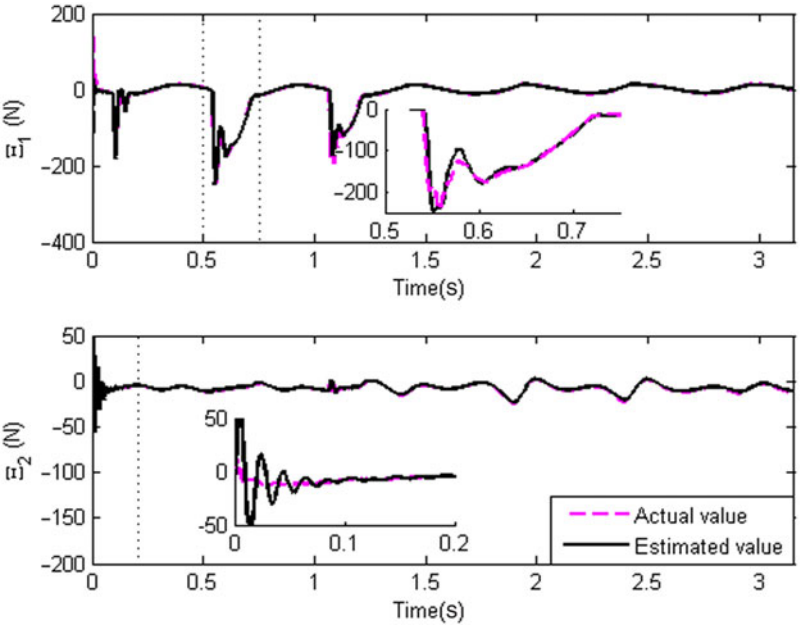


Fig. 18. Approximation of $\Xi(t)$.

7. Conclusion

A polynomial-based robust adaptive impedance controller for electrically driven robots has been proposed in this paper. The control law considers the actuator dynamics and has been derived under the assumption that no information of the system and environment is in hand. It has been assumed that the robot is actuated by permanent magnet DC motors. Moreover, it has been assumed that the desired trajectories do not include singular configurations that the Jacobian matrix is not invertible. According to the Stone–Weierstrass theorem, the universal approximation property of polynomials with degree N has been verified. The controller consists of two loops, the inner loop regulates motor currents and the outer loop is responsible for position control. The system stability has been verified by the Lyapunov second method. Simulation results on a 2DOF planar robot manipulator actuated by DC motors verify the effectiveness of the proposed controller.

https://doi.org/10.1017/S0263574720001009 Published online by Cambridge University Press

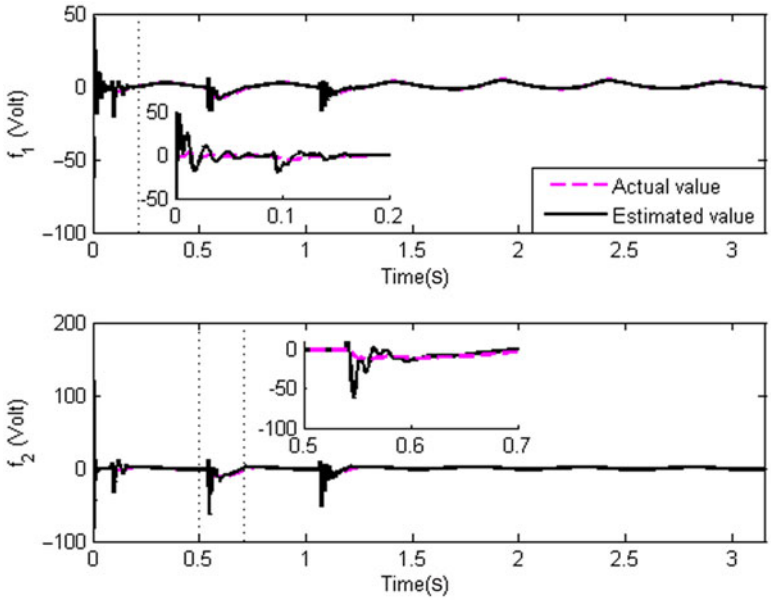


Fig. 19. Approximation of f.

8. Compliance with Ethical Standards

Authors declare that the manuscript has not been submitted to more than one journal for simultaneous consideration and it has not been published previously (partly or in full). In addition, this study has not been split up into several parts to increase the quantity of submissions. No data have been fabricated or manipulated to support the conclusions. Moreover, no data text, or theories by others are presented as if they were our own. Proper acknowledgements to other works have been given.

Disclosure of Potential Conflicts of Interest

Funding

No organization has funded this study.

Conflict of Interest

The authors declare that they have no conflicts of interest.

Research involving Human Participants and/or Animals

Authors declare that there has been no human participant or animal in this research.

Authors declare that there is no need for informed consent for this paper, since the results have been obtained using computer simulations.

References

1. R. Carloni, R. G. Sanfelice, A. R. Teel and C. Melchiorri, "A Hybrid Control Strategy for Robust Contact Detection and Force Regulation," *American Control Conference ACC 2007*, New York, NY, USA (2007) pp. 1461–1466.
2. J. J. Craig and M. H. Raibert, "A Systematic Method of Hybrid Position/Force Control of a Manipulator," *Proceedings of the Computer Software and Applications and* the IEEE Computer Society's Third International *Conference, COMPSAC 1979*, Chicago, IL, USA (1979) pp. 446–451.
3. A. Fanaei and M. Farrokhi, "Robust adaptive neuro-fuzzy controller for hybrid position/force control of robot manipulators in contact with unknown environment," *J. Intell. Fuzzy Syst.* **17**(2), 125–144 (2006).
4. M.-C. Chien and A. C. Huang, "Regressor-Free Adaptive Impedance Control of Flexible-Joint Robots Using FAT," **In:** *American Control Conference*, Minneapolis, MN, USA (2006) pp. 3904–3909, doi: 10.1109/ACC.2006.1657328.
5. J. J. Gonzalez and G. R. Widmann, "A force commanded impedance control scheme for robots with hard nonlinearities," *IEEE Trans. Control Syst. Technol.* **3**(4), 398–408 (1995).
6. S. Chan, B. Yao, W. Gao and M. Cheng, "Robust impedance control of robot manipulators," *Int. J. Robot. Automat.* **6**(4), 220–227 (1991).

https://doi.org/10.1017/S0263574720001009 Published online by Cambridge University Press

7. R. Bickel, M. Tomizuka and W. Chung, "Hybrid Impedance Control in Constraint Coordinates Using a Disturbance Observer," *Proceedings of the 35th IEEE Conference on Decision and Control*, Kobe, Japan (1996) pp. 1974–1979.
8. A. Jafari, R. Monfaredi, M. Rezaei, A. Talebi and S. S. Ghidary, "Sliding Mode Hybrid Impedance Control of Robot Manipulators Interacting With Unknown Environments Using VSMRC Method," **In:** *ASME 2012 International Mechanical Engineering Congress and Exposition*, Houston, Texas, USA (2012) pp. 1071–1081.
9. R. Anderson and M. W. Spong, "Hybrid impedance control of robotic manipulators," *IEEE J. Robot. Automat.* **4**, 549–556 (1988).
10. S. M. Ahmadi and M. M. Fateh, "Task-space control of robots using an adaptive Taylor series uncertainty estimator," *Int. J. Control* **92**(9), 2159–2169 (2018). doi: 10.1080/00207179.2018.1429673.
11. A. Izadbakhsh, S. Khorashadizadeh and P. Kheirkhahan, "Real-time fuzzy fractional-order control of electrically driven flexible-joint robots," *AUT J. Model.* Simulat. (2018), doi: 10.22060/MISCJ.2018.13523.5075
12. H. Chaoui, W. Gueaieb M. Biglarbegian and M. C. Yagoub, "Computationally efficient adaptive type-2 fuzzy control of flexible-joint manipulators," *Robotics* **2**(2), 66–91 (2013).
13. A. Izadbakhsh and P. Kheirkhahan, "An alternative stability proof for 'adaptive type-2 fuzzy estimation of uncertainties in the control of electrically flexible-joint robots'," *J. Vibr. Control* **25**(5), 977–983 (2019).
14. A. Izadbakhsh, S. Khorashadizadeh and S. Ghandali, "Robust adaptive impedance control of robot manipulators using Szasz-Mirakyan operator as universal approximator," *ISA Trans.* doi: 10.1016/j.isatra.2020.06.017
15. A. Izadbakhsh and S. Khorashadizadeh, "Robust impedance control of robot manipulators using differential equations as universal approximator," *Int. J. Control* **91**(10), 2170–2186 (2018).
16. A. Izadbakhsh, S. Khorashadizadeh and P. Kheirkhahan, "Tracking control of electrically driven robots using a model free observer," *Robotica* **37**(4), 729–755 (2019).
17. A. Izadbakhsh, "FAT-based robust adaptive control of electrically driven robots without velocity measurements," *Nonlinear Dyn.* **89**, 289–304 (2017).
18. A. Izadbakhsh, "A note on the 'nonlinear control of electrical flexible-joint robots'," *Nonlinear Dyn.* **89**, 2753–2767 (2017).
19. A. Izadbakhsh, "Robust adaptive control of voltage saturated flexible joint robots with experimental evaluations," *AUT J. Model. Simul.* **50**(1) (2017). doi: 10.1016/10.22060/miscj.2017.12174.5008
20. A. Izadbakhsh, H. Jabbari Asl and T. Narikiyo, "Robust Adaptive Control of Over-Constrained Actuated Cable-Driven Parallel Robots," **In:** *Cable-Driven Parallel Robots, CableCon 2019*, *Mechanisms and Machine Science* (A. Pott and T. Bruckmann, eds.), vol. 74 (Springer, Cham, 2019), pp. 209–220. doi: 10.1007/978-3-030-20751-9_18
21. M. C. Chien and A. C. Huang, "Adaptive impedance control of robot manipulators based on function approximation technique," *Robotica* **22**(4), 395–403 (2004).
22. A. Izadbakhsh and P. Kheirkhahan, "Adaptive fractional-order control of electrical flexible-joint robots: Theory and experiment," *Proc. Inst. Mech. Eng. I J. Syst. Control Eng.* **233**(9), 1136–1145 (2019).
23. A. Izadbakhsh and M. Masoumi, "FAT-Based Robust Adaptive Control of Flexible-Joint Robots: Singular Perturbation Approach," **In:** *Annual IEEE Industrial Society's 18th International Conference on Industrial Technology*, Toronto, ON, CA (2017) pp. 803–808, doi: 10.1109/ICIT.2017.7915462.
24. A. Izadbakhsh and S. Khorashadizadeh, "Robust adaptive control of robot manipulators using Bernstein polynomials as universal approximator," *Int. J. Robust Nonlinear Control* **30**(7), 2719–2735 (2020).
25. A. C. Huang, S. C. Wu and W. F. Ting, "A FAT-based adaptive controller for robot manipulators without regressor matrix: Theory and experiments," *Robotica* **24**(2), 205–210 (2006).
26. A. Izadbakhsh and P. Kheirkhahan, "A note on the 'task-space control of robots using an adaptive Taylor series uncertainty estimator'," *Int. J. Control* (2019). doi: 10.1080/00207179.2019.1614674
27. A. Izadbakhsh and P. Kheirkhahan, "On the voltage-based control of robot manipulators revisited," *Int. J. Control Automat. Syst.* **16**(4), 1887–1894 (2018).
28. Z. Chu, J. Cui and F. Sun, "Fuzzy adaptive disturbance-observer-based robust tracking control of electrically driven free-floating space manipulator," *IEEE Syst. J.* **8**(2), 343–352 (2014).
29. D. M. Dawson, Z. Qu and J. J. Carroll, "Tracking control of rigid-link electrically–Driven robot manipulators," *Int. J. Control* **56**(5), 991–1006 (1992).
30. A. Izadbakhsh and S. Khorashadizadeh, "Robust task-space control of robot manipulators using differential equations for uncertainty estimation," *Robotica* **35**(9), 1923–1938 (2017).
31. A. C. Huang and M. C. Chen, *Adaptive Control of Robot Manipulators: A Unified Regressor-Free Approach* (World Scientific Publishing Co. Pte. Ltd., Singapore, 2010).
32. A. Izadbakhsh, P. Kheirkhahan and S. Khorashadizadeh, "FAT-based robust adaptive control of electrically driven robots in interaction with environment," *Robotica* **37**(5), 779–800 (2019).
33. A. Izadbakhsh and S. Khorashadizadeh, "Single-loop PID controller design for electrical flexible-joint robots," *J. Braz. Soc. Mech. Sci. Eng.* **42**(2), 1–12 (2010).
34. Z. Qu and D. M. Dawson, *Robust Tracking Control of Robot Manipulators* (IEEE Press, Inc., New York, 1996).
35. A. Izadbakhsh and S. M. R. Rafiei, "Endpoint perfect tracking control of robots – A robust non inversion-based approach," *Int. J. Control Automat. Syst.* **7**(6), 888–898 (2009).

https://doi.org/10.1017/S0263574720001009 Published online by Cambridge University Press